ACS OMEGA

http://pubs.acs.org/journal/acsodf

Article

Fabrication and Characterization of Ag−Sr-Substituted Hydroxyapatite/Chitosan Coatings Deposited via Electrophoretic Deposition: A Design of Experiment Study

Osama Saleem,[§] Muhammad Wahaj,[§] Muhammad Asim Akhtar, and Muhammad Atiq Ur Rehman*

Cite This: *ACS Omega* 2020, 5, 22984−22992

Read Online

ACCESS | Metrics & More | Article Recommendations

ABSTRACT: In this study, silver−strontium-doped hydroxyapatite (AgSr-HA)/chitosan composite coatings were deposited on a 316L stainless steel (SS) substrate via electrophoretic deposition (EPD). The Taguchi design of experiment (DoE) approach was used to optimize the EPD parameters such as the applied voltage, interelectrode spacing, and deposition time. Furthermore, the concentration of AgSr-HA particles in the suspension was also optimized via the DoE approach. DoE results demonstrated that the "homogeneous" coatings were obtained at the deposition time of 7 min, deposition voltage of 20 V, and at a concentration of 5 g/L AgSr-HA particles in the suspension. Scanning electron microscopy (SEM), energy-dispersive X-ray spectroscopy (EDS), antibacterial studies, contact angle, and roughness measurements were performed to characterize the optimized coatings. SEM images confirmed the deposition of chitosan/AgSr-HA on the SS substrate. The wettability studies indicated the hydrophilic nature of the chitosan/AgSr-HA composite coatings, which confirmed that the developed coatings are suitable for biomedical applications, e.g., orthopedics. The average surface roughness of the chitosan/AgSr-HA composite coatings was in a suitable range used to attach the bone marrow stromal cells. Chitosan/AgSr-HA composite coatings showed an effective antibacterial effect against Gram-positive and Gram-negative bacteria. Moreover, the coatings developed apatite crystals on their surface upon immersion in simulated body fluid.

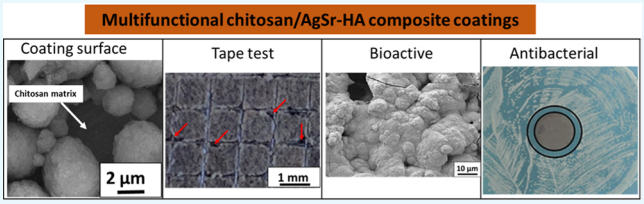

1. INTRODUCTION

To design orthopedic implants suitable to (i) bear the implantation load, (ii) improve binding ability with the natural bone, and (iii) resist the formation of biofilm, a wide range of composite coatings have been deposited on metallic substrates.[1,2] The present coating technology aimed to achieve coatings with multiple attributes such as biocompatibility, antibacterial activity, bioactivity, corrosion resistance, and wear resistance. However, to attain all of these attributes in a single coating system is a challenging task,[3−5] since the incorporation of antibacterial agents can impart antibacterial activity but at the same time, biocompatibility is compromised.[6] Therefore, there is a need to design a composition of the coating system that can maintain a balance between the two counteracting properties.[2]

Chitosan-based composite coatings have been deposited on metallic substrates, which has resulted in improved biocompatibility and bone binding ability for the implant.[7,8] Avcu et al.[2] have recently reviewed chitosan-based composite coatings deposited via electrophoretic deposition. Pishbin et al.[6] incorporated silver-doped bioactive glass in the chitosan matrix. It was shown that the coatings were antibacterial and bioactive. However, the cytotoxic effect attributed to the excessive release of Ag ions was a challenge. Similarly, chitosan/bioactive glass/gentamicin coatings were deposited on 316L stainless steel (SS), which resulted in bioactive and antibacterial effect.[5] It is important to mention that the excessive use of antibiotics has recently been declared as a global threat because the immune system of the body becomes resistant to particular drugs.[9] Therefore, metallic ions and natural herbs are widely considered as a safer option.[3,4] Moreover, the ability of chitosan to provide the local release of biologically active molecules at the site of injury facilitated the availability of a proper dose at the required site.[2] Recently, Akhtar et al.[10] deposited Cu(II)−chitosan complexes on 316L SS, which resulted in an antibacterial effect. Moreover, chitosan/hydroxyapatite (HA) coatings were deposited on an anodized titanium surface, which resulted in improved bioactivity and adhesion between the coatings and the substrate.[11] The available literature revealed that there is strong potential for the chitosan-based composite coatings to be applied in orthopedic applications.[12] Accordingly, this research work presents a significant advancement in the field by

Received: June 1, 2020
Accepted: July 31, 2020
Published: August 28, 2020

https://dx.doi.org/10.1021/acsomega.0c02582
ACS Omega 2020, 5, 22984−22992

deposition of co-substituted (Ag and Sr) HA/chitosan composite coatings. It was suggested that the incorporation of Sr is expected to enhance the bone binding ability of the implant[13−15] and the incorporation of Ag is expected to provide antibacterial effect.[16] Furthermore, the toxic effect associated with the release of silver ions may delay bone healing/binding,[17,18] which can be addressed by the addition of Sr along with silver in the HA complex. Thus, the Ag−Sr-substituted hydroxyapatite/chitosan composite coatings can provide antibacterial and bioactive effects in addition to the enhanced biocompatibility owing to chitosan.[19]

Electrophoretic deposition (EPD) is a two-stage colloidal processing technique, which allows depositing films at room temperature.[2,20] In the first stage, a stable suspension of the particles that are intended to be deposited is prepared. In the second stage, the charged particles/molecules move under the influence of an applied electric field.[21] EPD allows us to achieve uniform films independent of the substrate material and shape.[20] The factors that can affect the EPD process are pH, deposition time, electric field, the conductivity of the suspension, and concentration of particles.[22,23] The EPD process involving two or more components is a complex process.[20,24] Thus, the economical optimization of the EPD process is a challenging task. Therefore, Taguchi design of experiment (DoE) has recently been used for the development of controlled EPD processes to obtain homogenous coatings.[25−27] The Taguchi DoE approach allows to change more than one variable at a time, thus reducing the number of experiments to determine the optimum parameters. Traditionally, the one-variable-at-a-time approach has been used for process optimization. However, this approach is material and time-consuming. In contrast, DoE allows us to understand the effect of each variable on the output and the effect of one variable on another, thus improving the process reproducibility in addition to optimization with lesser number of experiments.[27]

One of the popular bioceramics is hydroxyapatite (HA), which has generated great interest as an advanced dental implant and orthopedic implant material.[28] HA is known for its biocompatibility, bioactivity, and osteoconductivity because it has chemical composition comparable with the human bone.[29,30] However, HA has poor mechanical properties that have been overcome by developing a composite of HA with various biopolymers (chitosan, alginate, poly(ether ether ketone) (PEEK), etc.),[30,31] i.e., a HA complex. Ca has also been substituted with various metallic ions to have a therapeutic effect.[32] For example, the incorporation of strontium improves the bioactivity of HA.[32] The incorporation of Zn, Ag, and Cu in HA is known to provide an antibacterial effect against a broad spectrum of bacteria.[33]

Here, we develop antibacterial coatings on a surgical grade 316L SS substrate via EPD. The EPD process was optimized via the Taguchi DoE approach to obtain coatings that have a maximum deposition yield with minimum standard deviation. Coatings obtained from the optimum EPD parameters and suspension compositions were fairly homogeneous with a coating thickness of ∼5 μm. The coatings presented suitable wettability and roughness for biomedical applications. Chitosan/AgSr-HA composite coatings showed an antibacterial effect against Gram-negative and Gram-positive bacteria.

2. MATERIALS AND METHODS

2.1. Suspension Preparation. To prepare the chitosan solution, 0.5 g/L chitosan (medium molecular weight with a 75−85% deacetylation degree, Sigma-Aldrich) was added to 1 vol % acetic acid (VWR International) and 20 vol % distilled water (ELGADV 25 PURELAB option R7BP) and then magnetically stirred for 30 min, which ensured complete dissolution of chitosan. Afterward, 79 vol % ethanol (absolute ethanol ≥99.8%, VWR International) was added to the prepared solution. The addition of ethanol can prevent the hydrolysis of water during the EPD process. It is important to note that 0.5 g/L concentration of chitosan was chosen based on suspension stability because if a higher concentration of chitosan is used, it may result in inhomogeneous coatings.[34]

2.2. Preparation of AgSr-HA/Chitosan Suspension. AgSr-HA/chitosan suspension was prepared by adding AgSr-HA (HA doped with 8 mol % Sr and 1 mol % Ag) to the prepared chitosan solution. The protocol of HA powder synthesis has already been published.[35] AgSr-HA was dispersed into the prepared chitosan solution with different concentrations, i.e., 1, 3, 5, and 7 wt % AgSr-HA. The suspension was magnetically stirred for 5 min and then ultrasonicated for 1 h to ensure uniform dispersion of solid particles, following the procedure of a previous study.[11]

2.3. Electrode Preparation. A 316L SS sheet was cut into dimensions of 3 × 2.5 cm^2 using a sheet cutter. The electrodes/substrates were then immersed in the mixture of ethanol and acetone for 5−10 min. Then, the electrodes were dried with hot air. It is important to mention that no further treatment was carried out to remove the oxide layer on the surface of the samples. For antibacterial studies, round samples with a 10 mm diameter were used.

2.4. EPD Setup. Briefly, 316L SS substrates were coated by chitosan/AgSr-HA via EPD to produce composite coatings. A two-electrode system was used for this purpose. 316L SS was chosen for both electrodes (anode and cathode) and the distance between the electrodes was kept at 1 cm. DC power supply (EX735M Multi-Mode PSU 75 V/150 V 300 W, Thurlby Thandar Instruments Limited) was used as a source of electrical connection. During the whole process, the current was continuously monitored using a multimeter (1906 Bench Digital Multimeter Thurlby Thandar Instruments Limited)

2.4.1. Taguchi Design of Experiment (DoE) Approach. A Taguchi array of experiments was formed for optimization of EPD parameters using Minitab17 software. An orthogonal Taguchi DoE array (L^{16} type) was constructed using three control factors (concentration of AgSr-HA in suspension (A), applied voltage (B), and deposition time (C)). Each had four levels, as illustrated in Table 1.

Table 1. Control Factors (Parameters) Along with Their Four Different Levels for the Deposition of Chitosan/AgSr-HA on 316L SS Substrate

symbol	control factors	level 1	level 2	level 3	level 4
A	concentration of AgSr-HA in the suspension (g/L)	1	3	5	7
B	applied voltage (V)	10	20	30	40
C	deposition time (min)	3	5	7	9

The control factors (concentration of AgSr-HA in the suspension, applied voltage, deposition, and deposition time) were varied according to the selected levels and their effect on the deposition yield (mass of chitosan/AgSr-HA composite coating) was taken into consideration. It should be noted that if the concentration of AgSr-HA in the suspension is more than 7

https://dx.doi.org/10.1021/acsomega.0c02582
ACS Omega 2020, 5, 22984−22992

Table 2. Experimentally Measured Values of Deposition Yield and the Corresponding Standard Deviation, S/N Ratio for the Deposition Yield, and S/N Ratio for the Standard Deviation for EPD of Chitosan/SrAg-HA Coatings

	control factors						
run	AgSr-HA concentration	voltage (V)	time (min)	deposition yield in g/cm^2	S/N ratio (dB)	standard deviation	S/N ratio (dB)
1	1	10	3	0.027273	−31.2853	0.005143	45.7757
2	1	20	5	0.028485	−30.9077	0.008176	41.7492
3	1	30	7	0.075758	−22.4114	0.011999	38.4171
4	1	40	9	0.074545	−22.5516	0.018953	34.4464
5	3	10	5	0.014545	−36.7457	0.005353	45.4281
6	3	20	3	0.032727	−29.7019	0.009271	40.6575
7	3	30	9	0.167879	−15.5001	0.009544	40.4054
8	3	40	7	0.189697	−14.4388	0.01487	36.5538
9	5	10	7	0.046061	−26.7333	0.01245	38.0966
10	5	20	9	0.165455	−15.6264	0.031422	30.0553
11	5	30	3	0.128485	−17.8230	0.033929	29.3886
12	5	40	5	0.273939	−11.2469	0.045426	26.8539
13	7	10	9	0.050909	−25.8641	0.008266	41.6541
14	7	20	7	0.207273	−13.6691	0.024529	32.2064
15	7	30	5	0.296364	−10.5635	0.067068	23.4697
16	7	40	3	0.227879	−12.8459	0.048704	26.2487

g/L, then sedimentation occurred, which detrimentally affected the stability of the suspension. On the other hand, the application of high voltages during EPD generates hydrogen gas bubbles at the surface of the substrate. According to Taguchi DoE, a total of 16 experimental runs were constructed, as shown in Table 2.

Each experiment was repeated thrice. Thus, 48 experiments were performed and the substrate was weighed before and after coating using a weighing balance (accurate up to 0.1 mg). After repeating each experiment three times, the average value of deposition yield, standard deviation, and signal to noise ratio(S/N) for deposition yield was calculated using eqs 1−3, respectively.[25,36,37]

$$\text{deposition yield} = \Delta\text{weight}/A \text{ in } \left(\frac{\text{mg}}{\text{cm}^2}\right) \quad (1)$$

where Δweight = weight after coating − weight before coating and A = area of the coating.

The desired coatings results were a higher deposition yield with lower values of standard deviation. S/N ratio for deposition yield was calculated using eq 2

$$\frac{\text{S}}{\text{N}} \text{ ratio of deposition yield} = -10 \log\left[\frac{1}{n}\left(\sum 1/y^2\right)\right] \quad (2)$$

where y = deposition yield and n = no. of observations.

The S/N ratio for the standard deviation was calculated using eq 3

$$\frac{\text{S}}{\text{N}} \text{ ratio of deposition yield} = -10 \log\left[\frac{1}{n}\left(\sum y^2\right)\right] \quad (3)$$

where y = standard deviation and n = no. of observations

2.5. Characterization of Chitosan/AgSr-HA Composite Coatings. The composite coatings were investigated for morphological and compositional analysis using a field-emission scanning electron microscope (FE-SEM) and an energy-dispersive X-ray spectroscope (EDS, S-4700 with a Noran System 7, Hitachi, Japan), respectively. The chemical composition of chitosan/AgSr-HA was assessed by attenuated total reflectance-Fourier transform infrared (ATR-FTIR) spectroscopy. FTIR analysis was conducted using an IRAffinity-1S Fourier transform infrared spectrometer (Shimadzu, Japan) equipped with a quest-ATR unit (diamond crystal). Intensity spectra were recorded in transmittance mode, with Happ−Genzel apodization, at 40 scans per spectrum, and a resolution of 4 cm^{-1}. The stability of the suspension and the charge on the particles were determined by ζ-potential measurements (Malvern Instruments, U.K.). For measuring the ζ-potential, the suspensions were diluted to 0.1 g/L (solid contents were kept at 0.1 g/L). The suspensions were diluted using ethanol. The surface properties of the coatings were evaluated by contact angle measurements that were carried out using a contact angle goniometer and the sessile drop technique was followed (DSA30 Kruess GmbH, Germany). Contact angle measurements were carried out on five samples and the mean values of the contact angle with the standard deviation are reported. A laser profilometer (UBM, Germany, ISC-2) was used to determine the surface roughness of the coated samples. A scanning velocity of 400 points per second and a measurement length of 5 to 7 mm were used in the UBM software to calculate the mean roughness (R_a). The qualitative adhesion strength between the coatings and the substrate was investigated by performing the tape test according to ASTM D3359 B-97. The experimental details have been published in our previous report.[37]

Antibacterial studies were conducted to evaluate the ability of the coatings to resist the attachment of bacteria. The agar disk diffusion method was followed to determine the antibacterial effect associated with the coatings. This antibacterial test was performed separately on two types of samples, namely, chitosan (control sample) and chitosan/AgSr-HA composite coatings. Before performing the test, it is important to sterilize the coatings for 1 h under ultraviolet (UV) light. Briefly, 20 mL of agar was filled in agar plates. Afterward, 20 μL of Luria−Bertani (LB) medium (Gram-negative (*Escherichia coli*) and Gram-positive (*Suberites carnosus*) bacteria) was added with an optical density (OD) of 0.015 at 600 nm. The LB medium was spread homogeneously on the surface of the agar. The next step was to place the coated sample on the prepared agar plates. Subsequently, agar plates were placed in the incubator for 24 h at 37 °C. After the incubation of 24 h, the inhibition zone was

https://dx.doi.org/10.1021/acsomega.0c02582
ACS Omega 2020, 5, 22984−22992

measured using "ImageJ" software (all of the tests were performed three times), according to previous studies.[3,4]

To determine the bone binding ability of the developed composite coatings, the coatings were immersed in 50 mL of simulated body fluid (SBF), as suggested by Kokubo et al.[38] The immersed coatings were placed in an orbital shaking incubator at 37 °C for 3 days. The SBF was refreshed every 24 h to maintain physiological conditions. After 3 days of incubation, the samples were removed, dried at room temperature, and assessed using SEM to determine the change in the morphology of the coatings.

3. RESULTS AND DISCUSSION

3.1. DoE Study of EPD of Chitosan/SrAg-HA. For optimization of the EPD parameters and suspension composition in terms of the intended application, i.e., bioactive and antibacterial coatings, the Taguchi DoE approach was used. Bioactivity and antibacterial effect are necessary for orthopedic applications (the intended application of this study). Bioactivity helps in bone growth, and the antibacterial effect resists the formation of a biofilm. In this approach, a higher deposition mass of the chitosan/AgSr-HA coatings with a low standard deviation was desired. A Taguchi array of L16 was designed for these three control factors, i.e., concentration, voltage, and deposition time. It is important to highlight that some other important parameters were not considered in this study. For example, ζ-potential, which relates to the stability, pH, and electric conductivity of the suspension, was not considered in this study since, in our previous studies, we optimized the ζ-potential of the suspension.[3] Thus, moving forward in the current study, we changed the concentration of AgSr-HA, since we aim to achieve bioactivity and antibacterial effect. Thus, it was necessary to study the effects of AgSr-HA concentration, applied voltage, and deposition time to achieve homogenous and thick coatings with a relatively high concentration of Ag−Sr HA, which helps in achieving bioactivity and antibacterial activity under physiological conditions. The 16 experiments were performed according to the conditions determined by the Taguchi array (Table 2), and the resulting deposition yield, the standard deviation in the deposition yield, S/N ratio for the deposition yield, and S/N ratio for the standard deviation were reported (Table 2). The experiments aimed to produce coatings with the maximum possible concentration of AgSr-HA in the suspension. Therefore, the composite coatings exhibit antibacterial (due to the presence of Ag) and bioactive (due to the presence of Sr and HA) effects. Moreover, coatings with fairly uniform microstructure are preferred.

The DoE approach offers to determine the effect of each parameter at different levels by averaging the mean value of deposition yield and its standard deviation, S/N ratios for deposition yield, and standard deviation. For example, the mean of deposition yield for factor A (concentration of AgSr-HA in the chitosan solution) was calculated by averaging the means of deposition yield for experiments 1−4 (A1), 5−8 (A2), 9−12 (A3), and 13−16 (A4). This method was used to determine the response values of S/N response of deposition yield and standard deviation, as illustrated in Tables 3 and 4.

The effects of these parameters on the deposition yield of chitosan/AgSr-HA composite coatings are shown graphically in Figure 1, which depicts that the mean of deposition yield is maximum for A4 (AgSr-HA concentration of 7 g/L), B4 (40 V applied voltage), and C2 (5 min deposition time) because these parameters show highest peaks, as shown in Figure 1A. The S/N ratio of the deposition yield was maximum at A4, B4, and C3 (7 min), as shown in Figure 1B. This provides no major difference between the results of the mean of deposition yield and S/N values of deposition yield. Moreover, it also shows that the deposition yield increases by increasing concentration and voltage according to Hamaker's law[20] (Figure 1). However, the deviation in Hamaker's law was observed with the increase in deposition time. It was observed from Figure 1A that if the deposition time is increased beyond 5 min, the deposition yield starts to decrease. The reason for this behavior could be that the maximum number of particles that can adhere to the substrate is reached at 5 min of deposition time and a further increase in deposition time causes the coating to fall into the suspension due to less cohesive force between the substrate and the coatings. Furthermore, the insulation effect of the coatings increases with the increase in the coating thickness, which renders a loss in conductivity associated with the substrate, and a further increase in deposition time may not yield an increase in coating mass following Hamaker's law.[39] Similar results have also been reported in the literature where the increase in deposition time led to a decrease in deposition mass.[26] Figure 1C shows the plot between the mean of standard deviation and EPD parameters. Since we desire to achieve coatings with the highest deposition yield and the lowest standard deviation, the coatings obtained from the parameters with the lowest standard deviation will be preferred. Figure 1C shows that the lowest standard deviation is achieved from A2 (concentration of AgSr-HA in the chitosan solution: 3 g/L), B1 (deposition voltage: 10 V), and C3 (deposition time: 7 min). Figure 1D shows that the S/N ratio for the standard deviation is appropriate for A4, B4, and C2. Combining the results of Figure 1C,D, it was inferred that the coatings produced from A4, B4, and C2 have higher statistical confidence and reproducibility. Since, statistically, S/N values are more important than the mean values, therefore, we consider A4, B4, and C2 as the "best" parameters on account of reproducibility. Now, combining the results of Figure 1A−D, it was inferred that the best parameters are A4, B4, and C2 in terms of the highest possible deposition yield with higher statistical confidence (reproducibility).

The maximum−minimum values for the S/N response of deposition showed that the voltage is the most important parameter (rank 1), followed by the deposition time and concentration of SrAg-HA in the chitosan solution (Table 3). This means that the S/N response of deposition yield is more sensitive to the voltage changes than the deposition time and concentration of AgSr-HA in the suspension.

Table 3. S/N (dB) Response for Deposition Yield

factors	level 1	level 2	level 3	level 4	maximum−minimum
concentration (g/L)	−26.79	−24.10	−17.86	−15.7	11.05
voltage (V)	−30.16	−22.48	−16.57	−15.27	14.89
time (min)	−22.91	−22.37	−19.31	−19.89	3.60

Table 4. S/N (dB) Response for Standard Deviation in Deposition Yield

factors	level 1	level 2	level 3	level 4	maximum−minimum
concentration (g/L)	40.10	40.76	31.10	30.89	9.87
voltage (V)	42.74	36.17	32.92	31.03	11.71
time (min)	35.52	34.38	36.32	36.64	2.27

https://dx.doi.org/10.1021/acsomega.0c02582
ACS Omega 2020, 5, 22984−22992

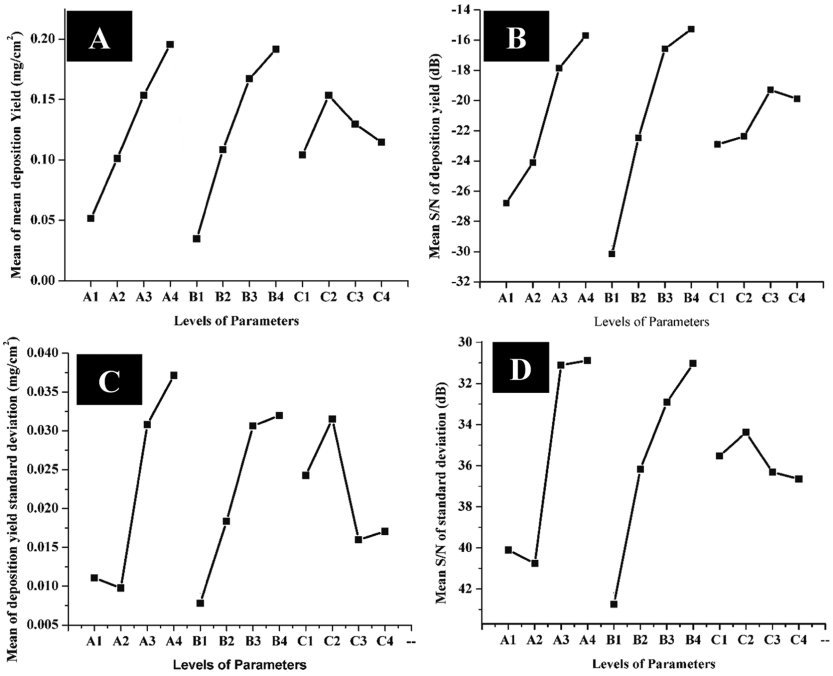

Figure 1. Effect of parameters on the deposition yield of chitosan/SrAg-HA coatings produced by EPD: (A) mean of mean deposition yield, (B) mean S/N for deposition yield, (C) means of deposition yield standard deviation, and (D) mean S/N for standard deviation.

The maximum−minimum values for the S/N response for standard deviation are reported in Table 4, which suggests that the applied voltage is the most significant parameter, which means that the standard deviation in the deposition yield is more sensitive to the changes in the applied voltage.

3.2. Adhesion Strength. The ability of the coatings to adhere to the substrate was evaluated qualitatively by the tape test. Figure 4 shows the results of the tape test for the chitosan/AgSr-HA composite coatings produced at a deposition voltage of 40 V, deposition time of 5 min, and concentration of 7 g/L AgSr-HA particles in the chitosan solution (best parameters elucidated by the DoE results). The total delaminated area was calculated using the ImageJ software, which elucidated that 5% of the coating was delaminated from the substrate, as shown by the red arrows in Figure 2. The adhesion strength was rated as

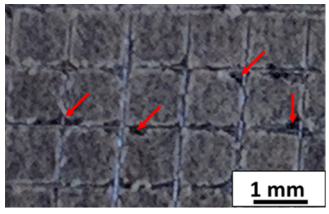

Figure 2. Digital image showing the result of the tape test for the chitosan/AgSr-HA composite coatings produced at a deposition voltage of 40 V and 5 min of deposition time from the suspension containing 7 g/L AgSr-HA particles dispersed in the chitosan solution.

"4B" according to the ASTM standard, which is suitable for orthopedic applications.[37] The tape test results confirmed the suitable adhesion between the coating and substrate; thus, we can conclude that the coatings can bear the implantation load. The reason for the good adhesion strength between the coating and substrate could be due to the encapsulation of HA in the chitosan matrix. Chitosan can be thought of as the glue adhering to the 316L SS substrate. Thus, the chitosan film can embed the HA particles in the matrix. Moreover, the relatively higher voltage (40 V) applied in this study provided sufficient energy to force the HA particles to the substrate and embed themselves into the chitosan matrix firmly enough to bear the implantation load. It is important to mention that the coatings produced at lower voltages showed poor adhesion strength (2B) with the substrate (images not shown here), which further shows that the voltage is the most significant parameter, as the increase in applied voltage significantly improved the adhesion strength between the coating and the substrate (predicted by the DoE results that voltage is the most significant parameter). Furthermore, we desire to have good bioactivity and antibacterial activity, which is associated with AgSr-HA particles. Thus, 7 g/L AgSr-HA is the best concentration considering the final application and the results of adhesion strength. The deposition time of 5 min gave the highest deposition yield, following Hamaker's law, and resulted in appropriate adhesion strength. This is the reason for performing morphological, compositional, and biological studies on the chitosan/AgSr-HA composite coatings produced at a deposition voltage of 40 V, deposition time of 5 min, and concentration of 7 g/L AgSr-HA particles in the chitosan solution.

3.3. Morphological Analysis. The statistical model suggested that the coatings obtained from A4 (concentration of AgSr-HA = 7 g/L), B4 (applied voltage = 40 V), and C2 (deposition time = 5 min) yield coatings with higher deposition yield and statistical confidence, i.e., reproducibility. Therefore, to validate and scrutinize the parameters suggested by the DoE, SEM analysis of the coatings was performed.

SEM analysis showed that the coatings produced from the best parameter predicted by DoE results were fairly homogenous (Figure 3). Figure 3A,B shows a homogenous distribution of AgSr-HA particles into the chitosan matrix. Figure 3B exhibits that the AgSr-HA particles were deposited individually and uniformly in the chitosan matrix. SEM image of the cross section showed a fairly uniform coating thickness of ∼5 μm (Figure 3C).

https://dx.doi.org/10.1021/acsomega.0c02582
ACS Omega 2020, 5, 22984−22992

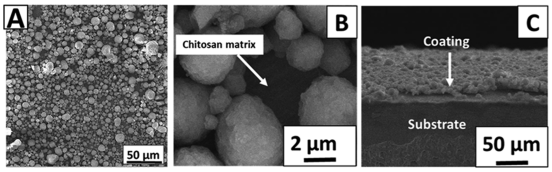

Figure 3. SEM images of chitosan/AgSr-HA coatings produced at a deposition voltage of 40 V and 5 min of deposition time from the suspension containing 7 g/L AgSr-HA at different magnifications: (A) image of the top surface at low magnification, (B) image of the top surface at high magnification, and (C) image of the cross section.

Similar results concerning the chitosan-based composite coatings have been reported in the literature.[5,11] According to the literature, there is no strict limit of coating thickness for promoting bone growth in orthopedic applications. Bioactivity is rather the function of the coating composition. Thus, due to this reason, the concentration of Ag−Sr HA in the deposited coatings was tuned. For example, Pishbin et al.[27] developed chitosan/bioactive glass coatings of 5−15 μm thickness for orthopedic application.

The deposition mechanism of chitosan/HA coatings has already been explained by Pawlick et al.[11] It was suggested that the positively charged chitosan molecules encapsulate the HA particles and move toward the cathode upon application of the electric field. In the present study, the chitosan/AgSr-HA suspension showed a ζ-potential of +30 ± 5 mV. The values of the ζ-potential obtained in the present study are in agreement with those in the literature.[11] The positive value of ζ-potential confirms the hypothesis of Pawlick et al.[26] Moreover, uniform coatings were obtained from a stable suspension of chitosan/AgSr-HA, as shown in Figure 2.

3.4. Compositional Analysis. Chitosan contains amino acids of high density.[34] The chemical formula for HA is $Ca_5(PO_4)_3(OH)$.[14] The EDX results confirm the presence of HA and chitosan in the composite coatings (EDX was carried out at the energy of 15 KV, and the working distance was 6 mm; Figure 4A). In the EDX pattern, the peaks of manganese (Mn), chromium (Cr), iron (Fe), and nickel (Ni) may arise from the SS substrate (due to the porous nature of the coatings and the high energy utilized for EDX analysis, i.e., 15 KV).[40] Calcium and phosphorous indicated the presence of HA. Furthermore, the peak of Ag and Sr may be attributed to the presence of co-substitute HA in the composite coatings. The presence of carbon refers to the chitosan in the composite coatings.[11]

Figure 4B shows the FTIR spectra of the chitosan/AgSr-HA composite coatings. The presence of chitosan was confirmed by the C═O stretching at 1718 cm^{-1}, N−H bending at 1575 cm^{-1}, −CH bending at 1344 and 1376 cm^{-1}, C−O−C stretching at 1152 cm^{-1}, and −C−O stretching at 1060 and 1030 cm^{-1} in the FTIR spectra of the chitosan/Ag−Sr HA composite coating. The presence of HA in the composite coating was confirmed by the O−P−O bending at 558 and 602 cm^{-1}, P−O stretching at 961 cm^{-1}, and P−O asymmetrical stretching at 1029 and 1089 cm^{-1}. It was observed that the N−H bending in pure chitosan coatings occurred at 1565 cm^{-1}, whereas, N−H bending in chitosan/AgSr-HA composite coating occurred at 1575 cm^{-1}. The slight shift in the N−H peak was due to the hydrogen bonding between the HA and chitosan.[41] The effect of Ag and Sr substitution was not observed in the FTIR spectra of the composite coatings, which is in agreement with the literature.[42]

3.5. Surface Properties. To determine the behavior of chitosan/AgSr-HA coatings in the physiological environment, the contact angle measurements were carried out using deionized water. The volume of the droplet was 5 μL. Surface wettability is important because, during the first few nanoseconds, water came in contact with the implant in the human body. Therefore, the role of surface wettability is important in determining the response of an implant in the human body.[43,44] The higher values of the contact angle (hydrophobic ∼90°) do not allow the cells to attach on the surface of the coatings. In contrast, lower values (hydrophilic >45°) of the contact angle do not allow the cells to spread on the surface of the coatings. Thus, ideally, the contact angle should neither be hydrophilic nor hydrophobic, rather, the contact angle should be ∼50° to support the attachment and proliferation of osteoblast cells.[34]

The contact angle measurements yielded a contact angle of 86 ± 2, 78 ± 3, and 50 ± 2° for the 316L SS substrate, chitosan coatings, and chitosan/AgSr-HA composite coatings, respectively. The wettability results suggest that the contact angle of chitosan/AgSr-HA composite coatings is less than that of chitosan coatings. The decrease in the contact angle refers to the hydrophilic nature of HA. A similar value for the contact angle measurements was reported in the literature for chitosan/HA coatings.[2,45] These findings suggest that the chitosan/AgSr-HA coatings presented suitable wettability for the protein attachment in the physiological conditions.[46]

To determine the suitability of the implant for applications related to the biomedical field, surface properties other than wettability are also important, for example, surface roughness and surface chemistry.[5,47] Therefore, to gain further information on the suitability of the chitosan/AgSr-HA composite coatings for biomedical applications, the average surface roughness of the 316L SS and chitosan/AgSr-HA composite coatings was measured. The surface roughness measurements yielded the average surface roughness of 0.2 ± 0.1 μm for 316L SS and 1.2 ±

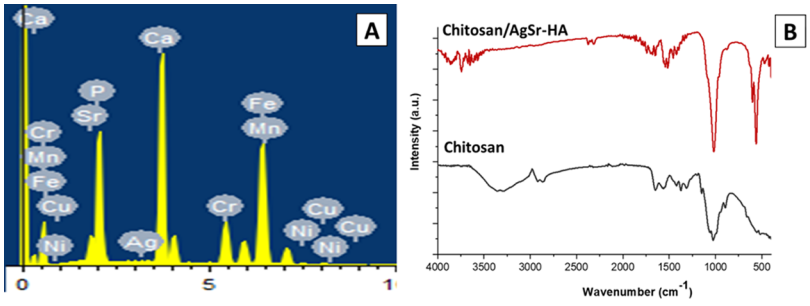

Figure 4. Compositional analysis of chitosan/AgSr-HA composite coatings deposited on 316L SS substrate. (A) energy-dispersive X-ray (EDX) analysis and (B) FTIR analysis.

https://dx.doi.org/10.1021/acsomega.0c02582
ACS Omega 2020, 5, 22984−22992

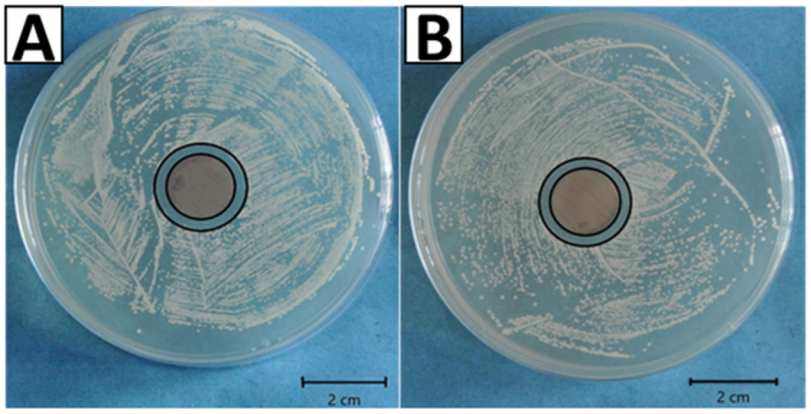

Figure 5. Inhibition halo tests for the chitosan/AgSr-HA composite coatings with (A) *E. coli* and (B) S. carnosus.

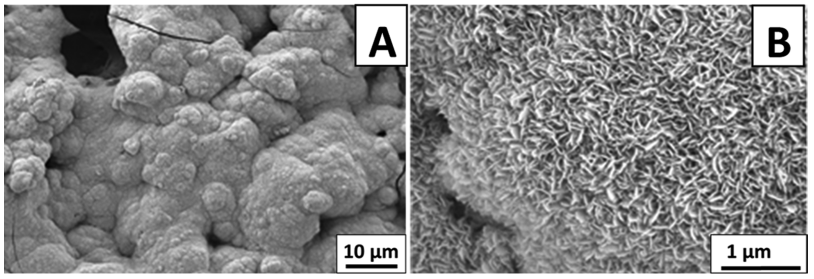

Figure 6. SEM images of the chitosan/AgSr-HA composite coatings after 3 days of immersion in SBF: (A) low-magnification image and (B) high-magnification image.

0.2 μm for chitosan/AgSr-HA coatings. EPD process causes a significant increase in the average surface roughness of the chitosan/AgSr-HA coatings. Similar observations were made in the literature, where it was shown that chitosan/HA coatings increased the surface roughness five times compared to that of the substrate.[45] Recently, Ureña et al.[48] showed that the average surface roughness in the range of 1.2−1.5 μm is favorable for the attachment and proliferation of bone marrow stromal cells (ST-2). Therefore, wettability and average roughness of chitosan/AgSr-HA coatings would be better for cells and protein attachment for bone regeneration applications.

3.6. Antibacterial Studies. Silver was substituted in HA to obtain an antibacterial effect. Thus, the effect of the release of silver ions under physiological conditions was evaluated for the antibacterial effect. The antibacterial effect of the chitosan/AgSr-HA coatings was determined by the agar disk diffusion test, as shown in Figure 5. The chitosan/AgSr-HA coatings developed a zone of inhibition around the sample against Gram-negative (*E. coli*) and Gram-positive (*S. carnosus*) bacteria. In contrast, chitosan coatings did not develop an inhibition zone (control sample, figure not shown here). The antibacterial effect of chitosan/AgSr-HA coatings was thus attributed to the release of silver ions from the HA complex. However, in this study, the release of silver ions was not evaluated quantitatively, thus leaving an important task for the future.

The antibacterial effect associated with chitosan/AgSr-HA was due to the release of silver ions from the chitosan matrix. The chitosan matrix has been shown to degrade in the physiological environment,[3] thereby causing the ions to release from the HA complex. The silver in the HA complex is usually in the metallic form, however, it changes to the ionic form upon exposure to the physiological medium.[4] The ionic silver is highly electropositive and highly reactive toward the electron donor species. It has been reported in the literature that the silver ions may cause the cytoplasm membrane to detach from the cell wall[49] and the morphology of the bacterial cell membranes was also shown to change due to the silver ions.[50] Moreover, the ionic silver may rupture the walls of the bacteria and enter the membrane, hindering the DNA replication activity, which may lead to the death of the bacteria.[9,49]

3.7. In Vitro Bioactivity. The ability of the chitosan/AgSr-HA composite coatings to bind with the natural bone was evaluated by immersing the coated samples in SBF for 3 days in an orbital shaking incubator. Figure 6 shows the apatite crystals formed on the surface of the coatings after three days of immersion in SBF. Figure 6A shows the "cauliflower-like" structure developed on the surface of the coatings, which is an indication of the development of apatite crystals on the surface of the coatings.[40] Apatite crystals appear to be quite dense covering the whole surface of the coatings. Figure 6B shows that the apatite crystals are nanoporous and highly dense. From the results, it is confirmed that the chitosan/AgSr-HA coatings are highly bioactive and have a strong ability to bind with the natural bone. The results obtained in the current study were in agreement with those in the literature.[51]

It is important to note that the addition of Sr in the HA complex significantly promotes the bone binding ability, as discussed in the literature.[14] The substitution of Ag in the HA complex is expected to delay the bone healing procedure (delayed formation of apatite crystals).[18] However, in the present scenario, the co-substitution of Sr along with the silver promoted the bone binding ability and the toxic effect associated with the release of Ag ions was mitigated. Thus, chitosan/AgSr-HA composite coatings provided antibacterial effect at the

https://dx.doi.org/10.1021/acsomega.0c02582
ACS Omega 2020, 5, 22984−22992

expense of Ag ions and bone binding ability at the expense of Sr ions.[19]

4. CONCLUSIONS

1. To optimize experimental parameters, the Taguchi DoE approach was used for chitosan/AgSr-HA composite coatings deposited on 316L SS via EPD. The suspension composition (concentration of AgSr-HA in the chitosan solution) and EPD parameters were optimized to get higher statistical confidence (reproducibility) and adhesion strength between the coatings and the substrate.
2. Chitosan/AgSr-HA composite coatings obtained from the optimum parameter showed uniform distribution of AgSr-HA particles in the chitosan matrix. The obtained coating thickness was ∼5 μm.
3. The presence of AgSr-HA in the coatings was confirmed by EDX and FTIR analyses.
4. Wettability and surface roughness studies confirmed that the chitosan/AgSr-HA coatings were suitable for biomedical applications.
5. The silver ion-release effect was traced by the antibacterial studies. Chitosan/AgSr-HA composite coatings showed the potent antibacterial effect against *S. carnosus* and *E. coli*.
6. In the SBF, chitosan/AgSr-HA composite coatings developed dense HA crystals on the surface of the coatings.

AUTHOR INFORMATION

Corresponding Author

Muhammad Atiq Ur Rehman − *Department of Materials Science and Engineering, Institute of Space Technology Islamabad, Islamabad 44000, Pakistan;* orcid.org/0000-0001-5201-973X; Email: atique1.1@hotmail.com

Authors

Osama Saleem − *Department of Materials Science and Engineering, Institute of Space Technology Islamabad, Islamabad 44000, Pakistan*

Muhammad Wahaj − *Department of Materials Science and Engineering, Institute of Space Technology Islamabad, Islamabad 44000, Pakistan*

Muhammad Asim Akhtar − *Institute of Biomaterials, Department of Material Science and Engineering, University of Erlangen-Nuremberg, 91058 Erlangen, Germany*

Complete contact information is available at: https://pubs.acs.org/10.1021/acsomega.0c02582

Author Contributions

[§]O.S. and M.W. contributed equally.

Notes

The authors declare no competing financial interest.

ACKNOWLEDGMENTS

M.A.U.R. is thankful to the HEC for the award of SRGP #2307. The authors would like to thank Fatih Erdem Bastan from Sakarya University,Turkey for free provision of HA.

REFERENCES

(1) Boccaccini, A.; Keim, S.; Ma, R.; Li, Y.; Zhitomirsky, I. Electrophoretic deposition of biomaterials. *J. R. Soc., Interface* **2010**, *7*, S581−S613.

(2) Avcu, E.; Baştan, F. E.; Abdullah, H. Z.; Rehman, M. A. U.; Avcu, Y. Y.; Boccaccini, A. R. Electrophoretic deposition of chitosan-based composite coatings for biomedical applications: A review. *Prog. Mater. Sci.* **2019**, *103*, 69−108.

(3) Ur Rehman, M. A.; Bastan, F. E.; Nawaz, Q.; Goldmann, W. H.; Maqbool, M.; Virtanen, S.; Boccaccini, A. R. Electrophoretic deposition of lawsone loaded bioactive glass (BG)/chitosan composite on polyetheretherketone (PEEK)/BG layers as antibacterial and bioactive coating. *J. Biomed. Mater. Res., Part A* **2018**, *106*, 3111−3122.

(4) Ur Rehman, M. A.; Ferraris, S.; Goldmann, W. H.; Perero, S.; Bastan, F. E.; Nawaz, Q.; Confiengo, G. G. d.; Ferraris, M.; Boccaccini, A. R. Antibacterial and Bioactive Coatings Based on Radio Frequency Co-Sputtering of Silver Nanocluster-Silica Coatings on PEEK/Bioactive Glass Layers Obtained by Electrophoretic Deposition. *ACS Appl. Mater. Interfaces* **2017**, *9*, 32489−32497.

(5) Pishbin, F.; Mouriño, V.; Flor, S.; Kreppel, S.; Salih, V.; Ryan, M. P.; Boccaccini, A. R. Electrophoretic deposition of gentamicin-loaded bioactive glass/chitosan composite coatings for orthopaedic implants. *ACS Appl. Mater. Interfaces* **2014**, *6*, 8796−8806.

(6) Pishbin, F.; Mourino, V.; Gilchrist, J.; McComb, D.; Kreppel, S.; Salih, V.; Ryan, M.; Boccaccini, A. R. Single-step electrochemical deposition of antimicrobial orthopaedic coatings based on a bioactive glass/chitosan/nano-silver composite system. *Acta Biomater.* **2013**, *9*, 7469−7479.

(7) Patel, K. D.; Singh, R. K.; Lee, J.-H.; Kim, H.-W. Electrophoretic coatings of hydroxyapatite with various nanocrystal shapes. *Mater. Lett.* **2019**, *234*, 148−154.

(8) Sorkhi, L.; Farrokhi-Rad, M.; Shahrabi, T. Electrophoretic Deposition of Hydroxyapatite−Chitosan−Titania on Stainless Steel 316 L. *Surfaces* **2019**, *2*, 458−467.

(9) Simchi, A.; Tamjid, E.; Pishbin, F.; Boccaccini, A. Recent progress in inorganic and composite coatings with bactericidal capability for orthopaedic applications. *Nanomedicine* **2011**, *7*, 22−39.

(10) Akhtar, A. M.; Ilyas, K.; Dlouhý, I.; Siska, F.; Boccaccini, R. A. Electrophoretic Deposition of Copper(II)−Chitosan Complexes for Antibacterial Coatings. *Int. J. Mol. Sci.* **2020**, *21*, No. 2637.

(11) Pawlik, A.; Rehman, M. A. U.; Nawaz, Q.; Bastan, F. E.; Sulka, G. D.; Boccaccini, A. R. Fabrication and characterization of electrophoretically deposited chitosan-hydroxyapatite composite coatings on anodic titanium dioxide layers. *Electrochim. Acta* **2019**, *307*, 465−473.

(12) Abdulkareem, M. H.; Abdalsalam, A. H.; Bohan, A. J. Influence of chitosan on the antibacterial activity of composite coating (PEEK/HAp) fabricated by electrophoretic deposition. *Prog. Org. Coat.* **2019**, *130*, 251−259.

(13) Aina, V.; Bergandi, L.; Lusvardi, G.; Malavasi, G.; Imrie, F. E.; Gibson, I. R.; Cerrato, G.; Ghigo, D. Sr-containing hydroxyapatite: morphologies of HA crystals and bioactivity on osteoblast cells. *Mater. Sci. Eng. C* **2013**, *33*, 1132−1142.

(14) Ni, G.; Lu, W.; Chiu, K.; Li, Z.; Fong, D.; Luk, K. Strontium-containing hydroxyapatite (Sr-HA) bioactive cement for primary hip replacement: An in vivo study. *J. Biomed. Mater. Res., Part B* **2006**, *77B*, 409−415.

(15) Ni, G.-X.; Yao, Z.-P.; Huang, G.-T.; Liu, W.-G.; Lu, W. W. The effect of strontium incorporation in hydroxyapatite on osteoblasts in vitro. *J. Mater. Sci.* **2011**, *22*, 961−967.

(16) Jelínek, M.; Kocourek, T.; Jurek, K.; Remsa, J.; Mikšovský, J.; Weiserová, M.; Strnad, J.; Luxbacher, T. Antibacterial properties of Ag-doped hydroxyapatite layers prepared by PLD method. *Appl. Phys. A* **2010**, *101*, 615−620.

(17) El-Rashidy, A. A.; Waly, G.; Gad, A.; Hashem, A. A.; Balasubramanian, P.; Kaya, S.; Boccaccini, A. R.; Sami, I. Preparation and in vitro characterization of silver-doped bioactive glass nanoparticles fabricated using a sol-gel process and modified Stöber method. *J. Non-Cryst. Solids* **2018**, *483*, 26−36.

(18) El-Rashidy, A. A.; Waly, G.; Gad, A.; Roether, J. A.; Hum, J.; Yang, Y.; Detsch, R.; Hashem, A. A.; Sami, I.; Goldmann, W. H. Antibacterial activity and biocompatibility of zein scaffolds containing silver-doped bioactive glass. *J. Biomed. Mater. Res.* **2018**, *13*, No. 065006.

(19) Huang, Y.; Zhang, X.; Zhang, H.; Qiao, H.; Zhang, X.; Jia, T.; Han, S.; Gao, Y.; Xiao, H.; Yang, H. Fabrication of silver-and strontium-doped hydroxyapatite/TiO2 nanotube bilayer coatings for enhancing bactericidal effect and osteoinductivity. *Ceram. Int.* **2017**, *43*, 992−1007.
(20) Besra, L.; Liu, M. A review on fundamentals and applications of electrophoretic deposition (EPD). *Prog. Mater. Sci.* **2007**, *52*, 1−61.
(21) Shi, Y.; Li, M.; Liu, Q.; Jia, Z.; Xu, X.; Cheng, Y.; Zheng, Y. Electrophoretic deposition of graphene oxide reinforced chitosan−hydroxyapatite nanocomposite coatings on Ti substrate. *J. Mater. Sci.: Mater. Med.* **2016**, *27*, No. 48.
(22) Jugowiec, D.; Łukaszczyk, A.; Cieniek, Ł.; Kowalski, K.; Rumian, Ł.; Pietryga, K.; Kot, M.; Pamuła, E.; Moskalewicz, T. Influence of the electrophoretic deposition route on the microstructure and properties of nano-hydroxyapatite/chitosan coatings on the Ti-13Nb-13Zr alloy. *Surf. Coat. Technol.* **2017**, *324*, 64−79.
(23) Farrokhi-Rad, M.; Fateh, A.; Shahrabi, T. Effect of pH on the electrophoretic deposition of chitosan in different alcoholic solutions. *Surf. Interface* **2018**, *12*, 145−150.
(24) Suo, L.; Jiang, N.; Wang, Y.; Wang, P.; Chen, J.; Pei, X.; Wang, J.; Wan, Q. The enhancement of osseointegration using a graphene oxide/chitosan/hydroxyapatite composite coating on titanium fabricated by electrophoretic deposition. *J. Biomed. Mater. Res., Part B* **2019**, *107*, 635−645.
(25) Pishbin, F.; Simchi, A.; Ryan, M.; Boccaccini, A. A study of the electrophoretic deposition of Bioglass suspensions using the Taguchi experimental design approach. *J. Eur. Ceram. Soc.* **2010**, *30*, 2963−2970.
(26) Atiq Ur Rehman, M.; Bastan, F. E.; Haider, B.; Boccaccini, A. R. Electrophoretic deposition of PEEK/bioactive glass composite coatings for orthopedic implants: A design of experiments (DoE) study. *Mater. Des.* **2017**, *130*, 223−230.
(27) Pishbin, F.; Simchi, A.; Ryan, M.; Boccaccini, A. Electrophoretic deposition of chitosan/45S5 Bioglass composite coatings for orthopaedic applications. *Surf. Coat. Technol.* **2011**, *205*, 5260−5268.
(28) Asri, R.; Harun, W.; Hassan, M.; Ghani, S.; Buyong, Z. A review of hydroxyapatite-based coating techniques: Sol−gel and electrochemical depositions on biocompatible metals. *J. Mech. Behav. Biomed. Mater.* **2016**, *57*, 95−108.
(29) Harun, W.; Asri, R.; Alias, J.; Zulkifli, F.; Kadirgama, K.; Ghani, S.; Shariffuddin, J. A comprehensive review of hydroxyapatite-based coatings adhesion on metallic biomaterials. *Ceram. Int.* **2018**, *44*, 1250−1268.
(30) Farrokhi-Rad, M.; Loghmani, S. K.; Shahrabi, T.; Khanmohammadi, S. Electrophoretic deposition of hydroxyapatite nanostructured coatings with controlled porosity. *J. Eur. Ceram. Soc.* **2014**, *34*, 97−106.
(31) Farrokhi-Rad, M.; Shahrabi, T.; Mahmoodi, S.; Khanmohammadi, S. Electrophoretic deposition of hydroxyapatite-chitosan-CNTs nanocomposite coatings. *Ceram. Int.* **2017**, *43*, 4663−4669.
(32) Gopi, D.; Shinyjoy, E.; Kavitha, L. Synthesis and spectral characterization of silver/magnesium co-substituted hydroxyapatite for biomedical applications. *Spectrochim. Acta, Part A* **2014**, *127*, 286−291.
(33) Šupová, M. Substituted hydroxyapatites for biomedical applications: a review. *Ceram. Int.* **2015**, *41*, 9203−9231.
(34) Avcu, E.; Yıldıran Avcu, Y.; Baştan, F. E.; Rehman, M. A. U.; Üstel, F.; Boccaccini, A. R. Tailoring the surface characteristics of electrophoretically deposited chitosan-based bioactive glass composite coatings on titanium implants via grit blasting. *Prog. Org. Coat.* **2018**, *123*, 362−373.
(35) Bastan, F.; Erdogan, G.; Moskalewicz, T.; Ustel, F. Spray drying of hydroxyapatite powders: The effect of spray drying parameters and heat treatment on the particle size and morphology. *J. Alloys Compd.* **2017**, *724*, 586−596.
(36) Rehman, M. A. U.; Munawar, M. A.; Nawaz, Q.; Anwar, M. Y. Design of Experiment Approach in the Industrial Gas Carburizing Process. In *Statistical Approaches With Emphasis on Design of Experiments Applied to Chemical Processes*; InTech: Rijeka, 2018; pp 99−113.
(37) Rehman, M. A. U.; Munawar, M. A.; Schubert, D. W.; Boccaccini, A. R. Electrophoretic deposition of chitosan/gelatin/bioactive glass composite coatings on 316L stainless steel: A design of experiment study. *Surf. Coat. Technol.* **2019**, *358*, 976−986.
(38) Kokubo, T.; Takadama, H. How useful is SBF in predicting in vivo bone bioactivity? *Biomaterials* **2006**, *27*, 2907−2915.
(39) Mahmoodi, S.; Sorkhi, L.; Farrokhi-Rad, M.; Shahrabi, T. Electrophoretic deposition of hydroxyapatite−chitosan nanocomposite coatings in different alcohols. *Surf. Coat. Technol.* **2013**, *216*, 106−114.
(40) Baştan, F. E.; Rehman, M. A. U.; Avcu, Y. Y.; Avcu, E.; Üstel, F.; Boccaccini, A. R. Electrophoretic co-deposition of PEEK-hydroxyapatite composite coatings for biomedical applications. *Colloids Surf., B* **2018**, *169*, 176−182.
(41) Nazeer, M. A.; Yilgör, E.; Yilgör, I. Intercalated chitosan/hydroxyapatite nanocomposites: Promising materials for bone tissue engineering applications. *Carbohydr. Polym.* **2017**, *175*, 38−46.
(42) Geng, Z.; Cui, Z.; Li, Z.; Zhu, S.; Liang, Y.; Liu, Y.; Li, X.; He, X.; Yu, X.; Wang, R.; et al. Strontium incorporation to optimize the antibacterial and biological characteristics of silver-substituted hydroxyapatite coating. *Mater. Sci. Eng., C* **2016**, *58*, 467−477.
(43) Bumgardner, J. D.; Wiser, R.; Elder, S.; Jouett, R.; Yang, Y.; Ong, J. Contact angle, protein adsorption and osteoblast precursor cell attachment to chitosan coatings bonded to titanium. *J. Biomater. Sci., Polym. Ed.* **2003**, *14*, 1401−1409.
(44) Menzies, K. L.; Jones, L. The impact of contact angle on the biocompatibility of biomaterials. *Optom. Vision Sci.* **2010**, *87*, 387−399.
(45) Karimi, N.; Kharaziha, M.; Raeissi, K. Electrophoretic deposition of chitosan reinforced graphene oxide-hydroxyapatite on the anodized titanium to improve biological and electrochemical characteristics. *Mater. Sci. Eng., C* **2019**, *98*, 140−152.
(46) Heise, S.; Wirth, T.; Höhlinger, M.; Hernández, Y. T.; Ortiz, J. A. R.; Wagener, V.; Virtanen, S.; Boccaccini, A. R. Electrophoretic deposition of chitosan/bioactive glass/silica coatings on stainless steel and WE43 Mg alloy substrates. *Surf. Coat. Technol.* **2018**, *344*, 553−563.
(47) Virk, R. S.; Rehman, M. A. U.; Boccaccini, A. R. PEEK based biocompatible coatings incorporating h-BN and bioactive glass by electrophoretic deposition. *ECS Trans.* **2018**, *82*, 89−95.
(48) Ureña, J.; Tsipas, S.; Jiménez-Morales, A.; Gordo, E.; Detsch, R.; Boccaccini, A. Cellular behaviour of bone marrow stromal cells on modified Ti-Nb surfaces. *Mater. Des.* **2018**, *140*, 452−459.
(49) Feng, Q. L.; Wu, J.; Chen, G.; Cui, F.; Kim, T.; Kim, J. A mechanistic study of the antibacterial effect of silver ions on *Escherichia coli* and *Staphylococcus aureus*. *J. Biomed. Mater. Res.* **2000**, *52*, 662−668.
(50) Jung, W. K.; Koo, H. C.; Kim, K. W.; Shin, S.; Kim, S. H.; Park, Y. H. Antibacterial activity and mechanism of action of the silver ion in *Staphylococcus aureus* and *Escherichia coli*. *Appl. Environ. Microbiol.* **2008**, *74*, 2171−2178.
(51) Vyas, V.; Kaur, T.; Kar, S.; Thirugnanam, A. Biofunctionalization of commercially pure titanium with chitosan/hydroxyapatite biocomposite via silanization: evaluation of biological performances. *J. Adhes. Sci. Technol.* **2017**, *31*, 1768−1781.

https://dx.doi.org/10.1021/acsomega.0c02582
ACS Omega 2020, 5, 22984−22992